DMD Fast Forward. Published on May 19, 2006 as doi:10.1124/dmd.106.009530

Title page

Predominant Contribution of Organic Anion Transporting Polypeptide OATP-B (OATP2B1) to Apical Uptake of Estrone-3-sulfate by Human Intestinal Caco-2 Cells*

Yoshimichi Sai, Yosuke Kaneko, Satsuki Ito, Keisuke Mitsuoka, Yukio Kato, Ikumi Tamai, Per Artursson, Akira Tsuji

Division of Pharmaceutical Sciences, Graduate School of Natural Science and Technology, Kanazawa University, Kakuma, Kanazawa, Japan (Y.S., Y.K., S.I., K.M., Y.K., A.T.); Department of Molecular Biopharmaceutics, Faculty of Pharmaceutical Sciences, Tokyo University of Science, Yamasaki, Noda, Japan (I.T.); Department of Pharmacy, Uppsala University (P.A.), P.O. Box 580, SE-751 23 Uppsala, Sweden (P.A.).

Running title:

Transport of Estrone-3-sulfate by OATP-B in Caco-2 cells

Correspondence
Ikumi Tamai, Ph.D., Prof.
Department of Molecular Biopharmaceutics, Faculty of Pharmaceutical Sciences, Tokyo University of Science, 2641 Yamasaki, Noda, Chiba 278-8510, Japan.
Tel:(81)-4-7121-3615/Fax:(81)-4-7121-3615/E-mail: tamai@rs.noda.tus.ac.jp

Document statistics
Number of text pages: 46
Number of tables: 2
Number of figures: 9
Number of references: 40
Number of words:
Abstract: 249
Introduction: 583
Discussion: 1296

Abbreviations:
BSP, sulfobromophthalein; DHEAS, dehydroepiandrosterone sulfate; FCCP, carbonylcyanide *p*-trifluoromethoxyphenyl hydrazone; HEPES, 4-(2-hydroxyethyl)-1-piperazineethanesulfonic acid; MES, 2-(*N*-morpholino)ethanesulfonic acid; PMSF, phenylmethanesulfonyl fluoride; DIDS, 4,4'-diisothiocyanostilbene-2-2'-disulfonic acid; HEK, human embryonic kidney.

DMD Fast Forward. Published on May 19, 2006 as DOI: 10.1124/dmd.106.009530
This article has not been copyedited and formatted. The final version may differ from this version.

ABSTRACT

Human organic anion transporting polypeptide OATP-B (OATP2B1) is a pH-sensitive transporter expressed in the apical membranes of small intestinal epithelial cells. In this study, we have examined the contribution of OATP-B to the uptake of [^{3}H]estrone-3-sulfate in Caco-2 cells in comparison with those of its homologues OATP-D (OATP3A1) and OATP-E (OATP4A1). Immunocytochemical study revealed that OATP-B is expressed in the apical membranes of Caco-2 cells. The uptake of [^{3}H]estrone-3-sulfate by Caco-2 cells was Na^+-independent and inhibited by several organic anions. It showed biphasic saturation kinetics, the Km values being 1.81 μM and 1.40 mM. The uptake of [^{3}H]estrone-3-sulfate by HEK293 cells stably expressing OATP-B (HEK293/OATP-B), was also Na^+-independent and inhibited by several organic anions. The Km value for estrone-3-sulfate uptake by OATP-B (1.56 μM) was close to that for the high-affinity component observed in Caco-2 cells. The mRNA expression level of OATP-B was higher than that of OATP-D or OATP-E in Caco-2 cells and in human jejunum biopsies from health volunteers. The values of [^{3}H]estrone-3-sulfate uptake normalized to OATP-B mRNA expression were similar in Caco-2 cells and HEK293/OATP-B cells. The specific activity of OATP-B per mRNA expression was much higher than that of OATP-D and OATP-E. [^{3}H]Estrone-3-sulfate uptake by membrane vesicles prepared from HEK293/OATP-B cells exhibited an overshoot phenomenon in the presence of

DMD Fast Forward. Published on May 19, 2006 as DOI: 10.1124/dmd.106.009530
This article has not been copyedited and formatted. The final version may differ from this version.

an inwardly directed H^+ gradient, suggesting that an H^+ gradient is the driving force of estrone-3-sulfate transport by OATP-B. These results suggest that OATP-B is predominantly responsible for the apical uptake of estrone-3-sulfate in Caco-2 cells.

DMD Fast Forward. Published on May 19, 2006 as DOI: 10.1124/dmd.106.009530
This article has not been copyedited and formatted. The final version may differ from this version.

INTRODUCTION

Organic anion transporting polypeptides (OATP, gene symbol *SLC21/SLCO*) are expressed in various organs and transport endogenous compounds, such as bile acids, peptides, conjugated metabolites and thyroid hormones, as well as xenobiotic compounds and clinically used therapeutic agents, such as pravastatin, benzylpenicillin and digoxin (Hsiang et al., 1999, Tamai et al., 2000a, Kullak-Ublick et al., 2001, Cui et al., 2001, Nakai et al., 2001). OATP-A (also called OATP1A2) was first isolated from human liver (Kullak-Ublick et al., 1995). Other members of the OATP family such as OATP-C (OATP2/LST-1/OATP1B1) (Hsiang et al., 1999, Abe et al., 1999), OATP8 (LST-2/OATP1B3) (Konig et al., 2000b, Abe et al., 2001), OATP-B (OATP-2B1), OATP-D (OATP3A1), OATP-E (OATP4A1) (Tamai et al., 2000a), OATP-F (OATP-1C1) (Pizzagalli et al., 2002), and prostaglandin transporter PGT (OATP2A1) (Lu et al., 1996) have also been identified in human. All of these transporters are thought to be involved in the disposition of anionic compounds in organs, except for OATP-R (OATP4C1), which was recently cloned, and efficiently transports digoxin and ouabain at the basolateral membranes of proximal tubule cells in the kidney (Mikkaichi et al., 2004).

Among them, OATP-B is localized at sinusoidal membrane of hepatocytes, like OATP-C and OATP8, and may play a role in hepatic uptake of organic anions (Kullak-Ublick et al., 2001, Konig et al., 2000a, 2000b). Compared with

DMD Fast Forward. Published on May 19, 2006 as DOI: 10.1124/dmd.106.009530
This article has not been copyedited and formatted. The final version may differ from this version.

OATP-C and OATP8, which are almost exclusively expressed in the liver, the tissue distribution of OATP-B is relatively ubiquitous (Tamai et al., 2000a). In placenta, OATP-B is localized at the basolateral membrane of the cytotrophoblast and is suggested to be involved in the transport of steroid hormones between the uterus and fetus (Ugele et al., 2003, St-Pierre et al., 2002). In the mammary gland, OATP-B is expressed in myoepithelium that surrounds the ductal epithelial cells, and is thought to transport estrogens to breast tumors and normal tissues (Pizzagalli et al., 2003). We have shown that OATP-B is also localized at the brush-border membrane of human small-intestinal epithelial cells, and transports estrone-3-sulfate and pravastatin in a pH-dependent manner (Kobayashi et al., 2003; Nozawa et al., 2004).

Because the microenvironment of epithelial cells in the small intestine is acidic, organic anions had been thought to be absorbed via the epithelial cells by passive diffusion according to the pH-partition hypothesis (Shiau et al., 1985). However, we established the existence of specific carrier-mediated absorption mechanisms for organic anions in the small intestine (Tamai et al., 1995, 1996, 1999, 2000b). OATP-B recognizes various types of organic anions as substrates and has a unique substrate specificity, with greater affinity for sulfate-conjugated compounds than non-conjugates (Kullak-Ublick et al., 2001; Tamai et al., 2001a). Therefore, recent identification of the pH-sensitive transporter OATP-B on intestinal brush-border membranes may imply a role in

the gastrointestinal absorption of organic anions. OATP-D and OATP-E are also expressed in the small intestine, as well as OATP-B, but information on the physiological and pharmacological significance of OATP-B is still limited.

In the present study, to clarify further the contribution of OATP-B to the transport of organic anions in the small intestine, we quantified the mRNA expression levels of OATP-B, OATP-D and OATP-E in human jejunum and human intestinal epithelial cell model Caco-2 cells and examined the subcellular localization of OATP-B protein in Caco-2 cells. In addition, by comparing the characteristics of estrone-3-sulfate uptake and the mRNA expression level of OATP-B in Caco-2 cells and in HEK293 cells stably expressing OATP-B, we evaluated the relative contribution of OATP-B to the uptake of estrone-3-sulfate from the apical surfaces of Caco-2 cells.

MATERIALS AND METHODS

Materials

[^{3}H]Estrone-3-sulfate ammonium salt (1.59 TBq/mmol) was purchased from PerkinElmer Life Science Products, Inc. (Boston, MA). The pcDNA3 vector was obtained from Invitrogen (Carlsbad, CA). HEK293 cells were obtained from the Japanese Cancer Research Resources Bank (Tokyo, Japan). Caco-2 cells were obtained from American Type Culture Collection (ATCC, Manassas, VA). All other reagents were purchased from Sigma Chemicals (St. Louis, MO) and Wako Pure Chemical Industries (Osaka, Japan).

Tissue samples

Human jejunal mucosa biopsies were obtained using a Watson capsule from 13 healthy volunteers (on no medication) aged 21 to 52 years (four females and nine males). Biopsies and all subsequent procedures were carried out with consent from the ethical review board of Huddinge University Hospital (Taipalensuu et al., 2001).

Cell Culture

HEK293 cells were routinely grown in Dulbecco's modified Eagle's medium containing 10% fetal calf serum (Life Technologies), benzylpenicillin, and streptomycin sulfate in a humidified incubator at 37 °C and 5% CO_2.

DMD Fast Forward. Published on May 19, 2006 as DOI: 10.1124/dmd.106.009530
This article has not been copyedited and formatted. The final version may differ from this version.

HEK293 cells were transfected with OATP-B subcloned into pcDNA3 or pcDNA3 vector alone according to the calcium phosphate precipitation method (Tamai et al., 2000a). To obtain HEK293 cells stably expressing OATP-B, cells grown on a 60 mm dish were transfected with 2 μg of plasmid encoding OATP-B. On the next day, the transfected cells were plated at a density of 2 x 10^5 cells/dish (100 mm). The cells were cultured in the presence of 1 mg/mL G418 (Sigma) and single colonies were isolated at day 14. The expression of OATP-B was screened by measuring the uptake of [^{3}H]estrone-3-sulfate. The established cells stably expressing OATP-B were named HEK293/OATP-B, and the cells expressing pcDNA3 were named HEK293/Mock cells. To obtain HEK293 cells transiently expressing OATP-B, OATP-D and OATP-E, each cDNA subcloned into pcDNA3 was transfected into HEK293 cells according to the calcium phosphate precipitation method (Tamai et al., 2000a). Determination of mRNA expression and transport activity was performed at 2 days after the transfection.

Caco-2 cells were cultured as described previously (Tavelin et al., 2002) with minor modifications. Caco-2 cells were routinely grown in Dulbecco's modified Eagle's medium containing 10% fetal calf serum (Life Technologies), benzylpenicillin, and streptomycin sulfate in 75 cm^2 flasks in a humidified incubator at 37 °C under 10% CO_2. When the cells reached confluence, they were plated on 2 cm^2 multi-well dishes at a density of 5 x 10^5 cells/well and the medium was changed at 3 hr after plating. The cells were cultured for 14-15

days before use for each experiment.

RT-PCR Analysis

Total RNAs from HEK293/OATP-B, HEK293/Mock, and Caco-2 cells were purified using an RNeasy® Mini Kit (QIAGEN) according to the manufacturer's instructions. After treatment of total RNA with DNase I, first strand cDNA was prepared from 5 μg of total RNA and amplified using OATP-B-specific primer pairs (5'- TCAAGCTGTTCGTTCTGTGC –3' and 5'-GTGTTCCCCACCTCGTTGAA –3'). These primers correspond to nucleotide positions 321-340 (sense) and 474-455 (antisense) of OATP-B cDNA. PCR reaction was run for 30 cycles of 94 °C for 30 sec, 55 °C for 30 sec and 72 °C for 30 sec. PCR products were separated by 2% agarose gel electrophoresis, followed by staining with ethidium bromide.

Immunoblot and Immunocytochemical Study of OATP-B in HEK293/OATP-B and Caco-2 Cells

Immunoblotting and Immunocytochemical staining were performed as described previously (Nozawa et al., 2002) with minor modifications. Rabbit polyclonal anti-OATP-B antiserum was prepared in our previous study using a synthesized carboxyl-terminal polypeptide of OATP-B with the amino acid sequence *C*LVSGPGKKPEDSRV as the epitope (Nozawa et al., 2002). This

sequence is specific for OATP-B, being absent in both OATP-D and OATP-E. The specificity of this antibody was confirmed in our previous study (Nozawa et al. (2002) Caco-2 cells were cultured on 15 mm micro cover glasses, and fixed with 10% formalin in PBS(-), 100% methanol on ice, and 0.1% Triton X-100 in PBS(-) at room temperature. The cells were incubated for 1 hr with polyclonal anti-OATP-B antiserum diluted 1:1,000 in PBS(-) containing 0.1% BSA or rabbit normal IgG. At the same time, monoclonal anti-Na^+/K^+-ATPase antibody diluted at 1:200 was mixed with the primary antibodies. After having been washed with PBS(-), the cells were incubated with Alexa Fluoro™ 594 goat anti-rabbit IgG and Alexa Fluoro™ 488 goat anti-mouse IgG (Molecular Probes, Inc., Eugene, OR) as the secondary antibodies, for 30 min. Then, they were mounted in VECTASHIELD mounting medium (Vector Laboratories) and examined with a confocal laser scanning microscope LSM510 (Carl Zeiss).

Transport Experiments in HEK293 cells and Caco-2 cells

HEK293/OATP-B and HEK293/Mock cells were cultured for 3 days on 15 cm dishes. They were harvested and suspended in an incubation medium [125 mM NaCl, 4.8 mM KCl, 5.6 mM D-glucose, 1.2 mM $CaCl_2$, 1.2 mM KH_2PO_4, 12 mM $MgSO_4$ and 25 mM HEPES-Tris (pH 7.4)]. The cell suspension was preincubated at 37 °C for 20 min in the incubation medium (pH 7.4), then centrifuged and the resultant cell pellets were mixed with the uptake medium (pH

6.0 or 7.4) containing a test compound to initiate uptake. The uptake medium contained the same constituents as the suspension medium except for 25 mM MES in place of HEPES, and was adjusted to pH 6.0 with Tris. In Na^+-free medium, NaCl was replaced with lithium chloride, potassium chloride, rubidium chloride, choline chloride or *N*-methylglucamine chloride. At appropriate times, aliquots of the mixture were withdrawn and the cells were separated from the uptake medium by centrifugal filtration through a layer of a mixture of silicone oil (SH550, Toray Dow Corning Co., Tokyo) and liquid paraffin (Wako Pure Chemical Industries) with a density of 1.03. Each cell pellet was solubilized in 3 N KOH and then neutralized with HCl. The cell-associated radioactivity was measured with a liquid scintillation counter using Cleasol-I as a liquid scintillation fluid (Nacalai Tesque, Kyoto, Japan).

Caco-2 cells were cultured on 2 cm^2 multi-well dishes for 14-15 days, then the transport experiments were performed. The cells were washed with incubation medium [137 mM NaCl, 5.4 mM KCl, 25 mM D-glucose, 0.95 mM $CaCl_2$, 0.44 mM KH_2PO_4, 0.81 mM $MgSO_4$ and 10 mM HEPES-Tris (pH 7.4)]. The cells were preincubated at 37 °C for 10 min in the incubation medium (pH 7.4), then the medium was aspirated and the uptake medium (pH 6.0 or pH 7.4) containing a test compound was added. Uptake medium contained the same constituents as the incubation medium except for 10 mM MES instead of HEPES, and was adjusted to pH 6.0 with Tris. In Na^+-free medium, NaCl was replaced

with lithium chloride, potassium chloride, rubidium chloride, choline chloride or *N*-methylglucamine chloride. At the designated times, the uptake medium was aspirated and the cells were washed with ice-cold incubation medium (pH 7.4). Each cell monolayer was solubilized in 5 N NaOH and then neutralized with HCl. The cell-associated radioactivity was measured with a liquid scintillation counter using Cleasol-I as a liquid scintillation fluid.

The content of protein in each cell was measured by the method reported by Bradford (1976) using a Bio-Rad protein assay kit. Initial uptake of [^{3}H]estrone-3-sulfate was determined at 2 min in both cell lines.

Quantitative RT-PCR Analysis

Quantification of the mRNAs coding for OATP-B, OATP-D and OATP-E was performed as described previously (Naruhashi *et al.*, 2002) by using LightCycler® technology (Roche Diagnostics). Total RNA was prepared as described below. The cDNA from 5 µg of RNA was used for OATP-B-, OATP-D- or OATP-E-specific PCR. Primer sets were as follows: OATP-B primers (5'- TCAAGCTGTTCGTTCTGTGC –3' and 5'- GTGTTCCCCACCTCGTTGAA –3'), OATP-D primers (5'- CTGCAACAGCACGAATCTCA –3' and 5'- AGGGATGAAGCCCAACAAAC –3') and OATP-E primers (5'- GAATACTAGGGGGCATCCCG –3' and 5'- GACGCCCAGCACCTTGTACA –3'), which produce 154, 265 and 170 bp

amplicons, respectively. The PCR programs were as follows: OATP-B: initial denaturation at 95 °C for 10 min, followed by 50 cycles of denaturation at 95 °C for 0 s and combined annealing extension at 56 °C for 0 s, 72 °C for 6 s. OATP-D: initial denaturation at 95 °C for 10 min, followed by 50 cycles of denaturation at 95 °C for 0 s and combined annealing extension at 56 °C for 0 s, 72 °C for 10 s. OATP-E: initial denaturation at 95 °C for 10 min, followed by 50 cycles of denaturation at 95 °C for 0 s and combined annealing extension at 56 °C for 0 s, 72 °C for 7 s. Each sample of cDNA was diluted with salmon sperm DNA to three different concentrations (i.e., 1, 4 and 16 ng/μL) for quantification. The standard curve for the real-time PCR analysis was generated by using gel-purified PCR products that had been quantified by measuring the UV absorbance (A_{260}) and diluted with salmon sperm DNA to 1 x 10^1 to 1 x 10^8 copy/μL. The copy number was calculated based on the conversion formulas: 1 A_{260} unit of ssDNA = 33 μg/mL H_2O, average molecular weight of cDNA = number of bases x 330 Da. The efficiency of the reverse-transcription was assumed to be 100%. mRNA expression is given as the copy number per unit RNA amount (copy/μg total RNA).

Transport Experiments in Membrane Vesicles

The membrane vesicles were prepared essentially as described previously (Tamai *et al.*, 2001b). Briefly, HEK293/OATP-B or HEK293/Mock

cells were cultured in the presence of 1 mg/mL G418. The confluent cells were harvested, washed, suspended in 25 mL of buffer I [10 mM NaCl, 1.5 mM $MgCl_2$, 0.02 mM PMSF and 10 mM HEPES-Tris (pH 7.4)], and placed on ice for 30 min. The cells were disrupted using a Nitrogen Bomb (Parr 4635) at 700 psi, homogenized, and separated by sucrose gradient centrifugation, and membrane vesicles were finally obtained as a pellet after centrifugation at 100,000 g for 3 hr. The final pellet was suspended in buffer II [250 mM sucrose, 0.02 mM PMSF and 10 mM HEPES-Tris (pH 7.4)] and stored at -80 °C until it was used. The content of protein in each preparation was measured by using a Bio-Rad protein assay kit. Transport studies were performed by a rapid filtration technique at 37 °C. Membrane vesicles stored at -80 °C were thawed rapidly at 37 °C and kept on ice. After the vesicles had been preincubated for 20 min at 37 °C, 10 µL of the membrane vesicle suspension containing 10 µg of protein was mixed with 90 µL of solution containing the test compound in buffer III [250 mM sucrose and 10 mM MES-Tris (pH 6.0) or HEPES-Tris (pH 7.4)] to initiate uptake reactions. The uptake was terminated by diluting the mixture with 1 mL of buffer IV [260 mM sucrose, 0.1 mM estrone-3-sulfate and 10 mM HEPES-Tris (pH 7.4)] at 4 °C, and the mixture was immediately filtered through a membrane filter (Millipore, GVWP02500, 0.22 µm pore size) that had been presoaked with a 0.1 mM estrone-3-sulfate solution overnight, and washed three times with buffer IV. The radioactivity retained on the membrane filter was quantitated with a

liquid scintillation counter. The background radioactivity was evaluated by mixing an ice-cold [^{3}H]estrone-3-sulfate solution with membrane vesicles that had previously been diluted with ice-cold buffer IV, immediately followed by filtration.

Data Analysis

All data are expressed as means ± SEM unless otherwise noted, and statistical analysis was performed with Student's *t*-test, taking $p < 0.05$ as the criterion of significance. Cell-to-medium (C/M) or vesicle-to-medium (V/M) ratio was obtained by dividing the cellular or vesicular uptake amount (mol/mg protein), respectively, by the concentration of test compound in the medium (mol/L). Kinetic parameters were estimated using either of the following equations, which consist of one or two saturable Michaelis-Menten components combined with a non-saturable component:

$$V = V_{max1} \times S / (K_{m1} + S) + V_{max2} \times S / (K_{m2} + S) + k_{ns} \times S \qquad (1)$$

$$V = V_{max} \times S / (K_m + S) + k_{ns} \times S \qquad (2)$$

where V, S, V_{max}, K_m, and k_{ns} represent the initial uptake velocity, substrate concentration, maximum uptake velocity, Michaelis constant, and non-saturable uptake clearance, respectively. The fitting was performed by nonlinear least-squares regression analysis using the MULTI program (Yamaoka et al., 1981). Validity of the model was verified based on Akaike's Information

Criterion (AIC).

RESULTS

mRNA Expression Levels of OATP-B, OATP-D and OATP-E in Human Jejunum and Caco-2 Cells

We quantitatively investigated the mRNA expression levels of OATPs in the human jejunum using biopsy samples from 13 healthy volunteers and Caco-2 cells (Table 1). Real-time quantitative PCR analysis was performed three times at different dilutions for each sample. The mRNA expression level of OATP-B was much higher than that of OATP-D or OATP-E in human jejunum ($p < 0.05$) and in Caco-2 cells. The mRNA expression level of villin, an epithelial cell-specific gene, was also measured to evaluate the relative content of epithelial cells. The villin-normalized mRNA expression level of OATP-B in human jejunum varied nine-fold from the lowest to the highest level, suggesting that there is considerable variation among individuals.

Subcellular Localization of OATP-B in Caco-2 Cells

OATP-B is localized at apical membranes of enterocytes in human small intestine (Nozawa et al., 2004). In the present study, therefore, localization of OATP-B in Caco-2 cells was examined using anti-OATP-B antibody. OATP-B was localized at the apical surface of Caco-2 cells, as shown by red staining in Fig. 1. In the control experiment with rabbit normal IgG, the signal was negligible (Fig. 1). Na^+/K^+-ATPase, a marker protein known to be localized at

DMD Fast Forward. Published on May 19, 2006 as DOI: 10.1124/dmd.106.009530
This article has not been copyedited and formatted. The final version may differ from this version.

the basal membrane of intestinal epithelial cells, was stained green, and there was no crossover signal with OATP-B (Fig. 1). These data suggest that OATP-B is predominantly localized at the apical membrane of Caco-2 cells.

Effect of Extracellular pH on Uptake of [^{3}H]Estrone-3-sulfate by HEK293/OATP-B and Caco-2 Cells

We compared the transport characteristics of OATP-B and those of Caco-2 cells in order to examine the possible involvement of this transporter in the uptake of estrone-3-sulfate by Caco-2 cells. For this purpose, we have established a cell line stably expressing OATP-B (HEK293/OATP-B). The expression of OATP-B was examined by RT-PCR and Western blot analysis. A band corresponding to OATP-B was observed in Caco-2 and HEK293/OATP-B cells, but not in HEK293/Mock cells (Fig. 2A). The expression of OATP-B protein was also observed in Caco-2 and HEK293/OATP-B cells (Fig. 2B).

First, the pH dependence of [^{3}H]estrone-3-sulfate uptake was compared between HEK293/OATP-B and Caco-2 cells. [^{3}H]Estrone-3-sulfate uptake by HEK293/OATP-B cells was much higher than that by HEK293/Mock cells, and the uptake was higher at pH 6.0 than at pH 7.4 (Figs. 3A and 3B). Unlabeled estrone-3-sulfate (100 μM) decreased the uptake of [^{3}H]estrone-3-sulfate in HEK293/OATP-B cells ($p < 0.05$) to the level of HEK293/Mock cells (Figs. 3A and 3B). On the other hand, [^{3}H]estrone-3-sulfate uptake by Caco-2 cells was

also inhibited by unlabeled estrone-3-sulfate (4 mM) ($p < 0.05$), and the uptake at pH 6.0 tended to be higher than that at pH 7.4, although the pH-dependence was not great (Figs. 3C and 3D).

Effect of Extracellular Cations on Uptake of [^{3}H]Estrone-3-sulfate by HEK293/OATP-B and Caco-2 Cells

Absence of Na^+-dependency is a well known characteristic of transport mediated by OATP-B. Therefore, we examined the Na^+-dependency to see whether the transport characteristics of Caco-2 cells matched those of OATP-B. Extracellular Na^+ was replaced with other cations (Li^+, K^+, Rb^+, choline$^+$ and *N*-methylglucamine$^+$), and the uptake of [^{3}H]estrone-3-sulfate was examined (Fig. 4). Replacement of extracellular cations had little effect on the uptake of [^{3}H]estrone-3-sulfate in both cell lines. Uptake was slightly decreased with choline and NMG, and this is consistent with the properties of other OATP family members (Hagenbuch et al., 2003).

Kinetic Analysis of [^{3}H]Estrone-3-sulfate Uptake by HEK293/OATP-B and Caco-2 Cells

Initial uptake rates of estrone-3-sulfate by HEK293/OATP-B cells at concentrations ranging from 4.7 nM to 15 μM exhibited saturation (Fig. 5A). Eadie-Hofstee plots showed a single straight line, the Km and Vmax values

being 1.56 ± 0.10 μM and 1.15 ± 0.04 nmol/mg protein/2 min, respectively (Fig. 5B). The Km value is similar to those reported by others (2-9 μM; Pizzagalli et al., 2003, Tamai et al., 2001a). On the other hand, biphasic saturation kinetics was observed when the initial uptake of estrone-3-sulfate by Caco-2 cells was examined at concentrations ranging from 4.7 nM to 4 mM (Figs. 5C and 5D), suggesting the presence of two kinetically distinct saturable components. The Km values of the high- and low-affinity sites were 1.81 ± 0.94 μM and 1.40 ± 0.01 mM, and the Vmax values were 0.134 ± 0.011 nmol/mg protein/2 min and 24.5 ± 1.1 nmol/mg protein/2 min, respectively (Figs. 5C and 5D). By comparing the values of the Vmax/Km ratio for high- and low-affinity sites, the contribution of the high-affinity site to overall uptake clearance was estimated to be approximately 4 times larger than that of the low-affinity site at low concentrations.

Inhibitory Effects of Various Compounds on Uptake of [^{3}H]Estrone-3-sulfate by HEK293/OATP-B and Caco-2 Cells

In order to compare substrate recognition specificity between Caco-2 and HEK293/OATP-B cells, the inhibitory effects of various compounds were examined. In addition to estrone-3-sulfate, OATP-B can transport BSP (sulfobromophthalein), DHEAS (dehydroepiandrosterone sulfate), pravastatin and benzylpenicillin (Tamai et al. 2000a, Kullak-Ublick et al., 2001, Nozawa et al.,

2004). Therefore, the IC_{50} values of those four compounds were examined. The [^{3}H]estrone-3-sulfate uptake by HEK293/OATP-B and Caco-2 cells was strongly inhibited by BSP and DHEAS, both of which are sulfate conjugates (Fig. 6, Table 2). Pravastatin and benzylpenicillin also inhibited the uptake of [^{3}H]estrone-3-sulfate in both HEK293/OATP-B and Caco-2 cells (Fig. 6). The IC_{50} values for DHEAS, pravastatin and benzylpenicillin were similar in HEK293/OATP-B and Caco-2 cells, while that for BSP exhibited a 10-fold difference (Table 2). These IC_{50} values are not very different from the reported Km values for transport of BSP (0.7 μM), DHEAS (9 μM) and pravastatin (2 mM) by OATP-B (Kullak-Ublick et al., 2001, Pizzagalli et al., 2003, Nozawa et al., 2004). In addition, the uptake of [^{3}H]estrone-3-sulfate was inhibited by several organic anions and monocarboxylic acids, but not by organic cations except cimetidine (Fig. 7). The inhibition profiles were similar for HEK293/OATP-B and Caco-2 cells (Fig. 7).

Transport of [^{3}H]Estrone-3-sulfate Observed in Caco-2 Cells Can Be Accounted for by OATP-B's Expression Level and Intrinsic Transport Activity

In order to know whether OATP-B can account for the observed [^{3}H]estrone-3-sulfate transport activity in Caco-2 cells, we next examined (i) the mRNA copy number of OATP-B in Caco-2 cells and (ii) the linearity of the

relationship between OATP-B mRNA expression level and [^{3}H]estrone-3-sulfate transport activity. HEK293 cells were transiently transfected with different amounts of OATP-B cDNA plasmids, and using the same batch of transfectants, the relationship between mRNA expression and initial uptake clearance of [^{3}H]estrone-3-sulfate was examined (Fig. 8). The transport activity in HEK293 cells was increased (9.75-348 µL/mg protein/min) with increase in the transfected amount of OATP-B cDNA (1-20 µg/culture dish) (Fig. 8). A double logarithmic plot of initial uptake clearance of [^{3}H]estrone-3-sulfate vs. mRNA expression of OATP-B in HEK293 cells was linear within the range of 3,200-91,800 copy/ng total RNA) (Fig. 8). Based on this correlation, OATP-B mRNA expression in Caco-2 cells (9,030 copy/ng total RNA) can account for about 20-30 µL/mg protein/min of initial uptake clearance, which was close to the actual uptake activity observed in Caco-2 cells (17.2 µL/mg protein/min, Fig. 8, broken line, and the Vmax/Km value of the high-affinity site (37.0 µL/mg protein/min, Fig. 5C,D)). Moreover, as Caco-2 cells express OATP-D (34.9 copy/ng total RNA) and OATP-E (154 copy/ng total RNA) (Table 1), the contributions of those transporters to the [^{3}H]estrone-3-sulfate uptake were also assessed. When HEK293 cells were transfected with plasmid encoding OATP-D cDNA, the [^{3}H]estrone-3-sulfate uptake by the cells was as small as the non-saturable endogenous transport activity of non-transfected HEK293 cells (3.02 µL/mg protein/min), although 69,200 copy/ng total RNA of OATP-D

mRNAs was expressed in the transfected cells (Fig. 8, triangle). In the case of OATP-E transfection, the uptake activity and mRNA expression level were 10.8 μL/mg protein/min and 30,200 copy/ng total RNA, respectively (Fig. 8, square). The uptake activity of OATP-E-transfected cells was much smaller than that via OATP-B, even when the mRNA expression levels for both OATPs were comparable (Fig. 8). Considering the relatively low transport activity per mRNA copy in HEK293 cells, and the very low mRNA expression level in Caco-2 cells, neither OATP-D nor OATP-E can be a major transporter for [^{3}H]estrone-3-sulfate uptake in Caco-2 cells. These results suggest that OATP-B, but not OATP-D or OATP-E, is the predominant contributor to estrone-3-sulfate uptake by Caco-2 cells.

Transport of [^{3}H]Estrone-3-sulfate by OATP-B Depends on an H^+-Gradient

Uptake of [^{3}H]estrone-3-sulfate by membrane vesicles expressing OATP-B was examined. In the presence of an inwardly directed H^+-gradient (pH_{out}/pH_{in} = 6.0/7.4), the uptake of [^{3}H]estrone-3-sulfate by OATP-B-vesicles was much higher than that by Mock-vesicles ($p < 0.05$) and showed an overshoot phenomenon (Fig. 9A). The overshoot uptake was not observed in the presence of an H^+-ionophore, FCCP (Fig. 9A). In the absence of the H^+-gradient (pH_{out}/pH_{in} = 7.4/7.4), no overshoot uptake of [^{3}H]estrone-3-sulfate was observed in both OATP-B- or Mock-vesicles (Fig. 9B). The osmolarity of

the medium was changed (290-1,090 mOsm/kg) by increasing the concentration of sucrose, and the uptake of [^{3}H]estrone-3-sulfate in the steady state was examined. Uptake of [^{3}H]estrone-3-sulfate at 120 min by membrane vesicles prepared from OATP-B- and mock-transfected HEK293 cells decreased linearly as the reciprocal of medium osmolarity decreased, suggesting that [^{3}H]estrone-3-sulfate is taken up into an intravesicular space (data not shown).

DISCUSSION

Although OATP-B is known to be localized at apical membranes of human small intestinal epithelial cells, it has not yet been clarified whether this transporter plays physiological/pharmacological roles as an uptake mechanism in the intestinal absorption of its substrates or not. In this study, we characterized the estrone-3-sulfate uptake at the apical membranes of human intestinal Caco-2 cells and compared it with the OATP-B-mediated transport. The expression of OATP-B in Caco-2 cell was clarified by RT-PCR and Western blot analysis (Fig. 2). OATP-B was localized at the apical membrane of Caco-2 cells (Fig. 1). The present findings, as well as the previous observation that OATP-B is localized at the brush-border membrane of human enterocytes (Kobayashi et al., 2003) support the hypothesis that OATP-B plays an important role in the uptake of its substrates at the luminal membranes of the small intestine. The characteristics of estrone-3-sulfate uptake at the apical membranes of human intestinal Caco-2 cells were quite similar to those of HEK293/OATP-B cells in terms of i) the inhibition profile by various kinds of organic anions, monocarboxylic acids (Fig. 7), ii) the IC50 values of BSP, DHEAS, pravastatin and benzylpenicillin (Fig. 6, Table 2), iii) the Km value (Fig. 5), iv) the effect of replacement of extracellular cations (Fig. 4), and v) the specific activity per mRNA expression (Fig. 8) OATP-B was the most abundant transporter among the OATPs expressed in the small intestine and Caco-2 cells

(Table 1 and Fig. 8). All of these data suggested that OATP-B plays a predominant role in the uptake of estrone-3-sulfate at the luminal membranes of the small intestine.

There was a marked difference in the expression levels of OATPs between human jejunum and Caco-2 cells. There are several possible explanations for the difference. Firstly, the relative content of epithelial cells in the human biopsy samples could be lower than that in Caco-2 cell samples: as OATPs are expressed only in the absorptive epithelial cells, contamination of non-epithelial cells in the biopsy sample would decrease the apparent expression level of OATPs. However, as the expression levels of villin, an epithelial cell-specific gene, are comparable in the biopsy sample (661 copy/ng total RNA) and in Caco-2 cells (925 copy/ng total RNA), contamination seems unlikely to account for the difference. Secondly, up-regulation or down-regulation of OATPs either in Caco-2 cells or in the biopsy samples may explain the difference. Indeed, there was a several-fold variation in the expression level of OATP-B among our Caco-2 cell cultures (data not shown), even though the [^{3}H]estrone-3-sulfate uptake activity and OATP-B mRNA expression level were well correlated. Thirdly, mRNAs of OATPs are not evenly distributed longitudinally along the intestine, so for instance, mRNA expression of OATP-B in the jejunum could be lower than in other parts. For example, mRNA and protein expression of the Na^+-dependent bile acid transporter ASBT

is restricted to the terminal ileum (Saeki et al., 1999, Stelzner et al., 2000). Recently, Sun et al. examined gene expression of several transporters and metabolic enzymes, such as cytochrome P450, in Caco-2 cells, and found that it differed from the expression profile in human small intestine (Sun et al., 2002). In addition, expression of constitutive genes in Caco-2 cells could depend on the culture conditions. Further *in vivo* and *in vitro* analyses would be necessary to examine these possibilities.

The transport by OATP-B is pH-sensitive, with the uptake of estrone-3-sulfate, pravastatin, DHEAS, taurocholic acid and fexofenadine being increased at acidic pH compared with neutral pH (Kobayashi et al., 2003, Nozawa et al., 2004). In this study, the uptake of estrone-3-sulfate by HEK293/OATP-B cells was also higher at pH 6.0 than at pH 7.4 (Fig. 3). Because OATP-B-mediated transport was reported to be inhibited by the proton-ionophore FCCP, protons may be a candidate for the driving force of transport by OATP-B (Nozawa et al., 2004). To clarify whether or not the proton gradient is indeed the driving force for OATP-B, we here performed transport studies using membrane vesicles expressing OATP-B (Fig. 9). An overshoot phenomenon, which was inhibited by FCCP, was observed in the presence of an inwardly directed gradient of protons, suggesting that estrone-3-sulfate uptake is driven, at least in part, by the proton gradient. This characteristic could be favorable for OATP-B to play a physiological role in the uptake of substrates at

the intestinal lumen.

The pH dependence of estrone-3-sulfate uptake by Caco-2 cells was not large, compared with that seen in HEK293/OATP-B cells (Figs. 3, 4). There are several possible reasons for such a difference. First, some other transport mechanism may also exist in the apical membranes of Caco-2 cells and could be involved in uptake of estrone-3-sulfate. We examined the expression and possible involvement of OATP-D and OATP-E, both of which are expressed in the small intestine and Caco-2 cells (Tamai et al., 2000a, Fig. 8, Table 1). HEK293 cells transfected with OATP-D and OATP-E exhibited much lower estrone-3-sulfate uptake than did the cells transfected with OATP-B (Fig. 8): the expression levels of OATP-D and OATP-E transiently transfected in HEK293 cells were approximately 1,000- and 400-fold higher, respectively, than in Caco-2 cells, whereas uptake of estrone-3-sulfate was lower than that observed in Caco-2 cells in each case (Fig. 8). These results suggest that OATP-D and OATP-E do not contribute substantially to apical uptake of estrone-3-sulfate by Caco-2 cells. Another possible reason for the discrepancy in pH dependence between HEK293/OATP-B and Caco-2 cells may be a difference in the microclimate pH in the vicinity of OATP-B proteins in Caco-2 cells. An isoform of Na^+/H^+ exchanger, NHE3, is expressed in the apical membrane of Caco-2 cells (Janecki et al., 1998). This protein could release protons close to OATP-B, resulting in a constant supply of protons as a driving force of OATP-B. Indeed,

NHE3 affects transport activity of oligopeptide transporter PEPT1 by supplying a driving force at the apical membrane of Caco-2 cells (Walker et al., 1998, Thwaites et al., 2002, Watanabe et al., 2005).

Estrone-3-sulfate is a sulfate-conjugated metabolite of estrone and acts as a carrier of estrogen in plasma and various tissues. Estrone is metabolized to estrone-3-sulfate in the liver, and estrone-3-sulfate is secreted into bile, reabsorbed into enterocytes, and undergoes enterohepatic circulation (Honjo 1979). Because estrone-3-sulfate is likely to exist in ionic form at physiological pH, it is thought that carrier-mediated transport systems play a major role in the membrane permeation processes involved. While hepatic uptake of estrogen may be mediated by OATP family member(s) expressed in the sinusoidal membranes of hepatocytes (König et al., 2000), intestinal uptake of estrogen has not been well characterized. The results in this study suggest that intestinal absorption of estrogen in humans is likely to be mediated by OATP-B. It is an interesting hypothesis that intestinal OATP-B not only accepts estrone-3-sulfate as an endogenous substrate, but also recognizes therapeutic agents such as pravastatin and benzylpenicillin, contributing to their oral absorption (Kobayashi et al., 2003).

In conclusion, we have established that OATP-B is expressed in apical membranes of Caco-2 cells, and that it is the predominant contributor to apical uptake of estrone-3-sulfate, based on the kinetic parameters of the uptake, the

inhibitory profiles of various substrates, and the linear relationship between mRNA expression levels and transport activity. Inter-individual variation in the mRNA expression level of OATP-B in the human jejunum was large. Genetic polymorphisms of OATP-B were previously found and there were allelic differences of transport activity for estrone-3-sulfate (Nozawa et al., 2002; Ishikawa et al., 2004). Therefore, further analysis is required to examine the pharmacokinetic and/or pharmacodynamic impact of such polymorphisms in OATP-B to clarify fully the functional importance of this transporter in intestinal transport of endogenous compounds and various xenobiotics. Recently, citrus juices have been reported to reduce the bioavailability of orally administered fexofenadine. OATP-B may be of importance as a target for individualized medicine.

REFERENCES

Abe T, Kakyo M, Tokui T, Nakagomi R, Nishio T, Nakai D, Nomura H, Unno M, Suzuki M, Naitoh T, Matsuno S and Yawo H (1999) Identification of a novel gene family encoding human liver-specific organic anion transporter LST-1. *J Biol Chem* **274**:17159-17163.

Abe T, Unno M, Onogawa T, Tokui T, Kondo TN, Nakagomi R, Adachi H, Fujiwara K, Okabe M, Suzuki T, Nunoki K, Sato E, Kakyo M, Nishio T, Sugita J, Asano N, Tanemoto M, Seki M, Date F, Ono K, Kondo Y, Shiiba K, Suzuki M, Ohtani H, Shimosegawa T, Iinuma K, Nagura H, Ito S and Matsuno S. (2001) LST-2, a human liver-specific organic anion transporter, determines methotrexate sensitivity in gastrointestinal cancers. *Gastroenterology* **120**:1689-1699.

Adachi H, Suzuki T, Abe M, Asano N, Mizutamari H, Tanemoto M, Nishio T, Onogawa T, Toyohara T, Kasai S, Satoh F, Suzuki M, Tokui T, Unno M, Shimosegawa T, Matsuno S, Ito S and Abe T (2003) Molecular characterization of human and rat organic anion transporter OATP-D. *Am J Physiol* **285**:F1188-F1197.

Bradford MM (1976) A rapid and sensitive method for the quantitation of microgram quantities of protein utilizing the principle of protein-dye binding. *Anal Biochem* **72**:248-254.

Cui Y, Konig J, Leier I, Buchholz U and Keppler D (2001) Hepatic uptake of

bilirubin and its conjugates by the human organic anion transporter SLC21A6. *J Biol Chem* **276**:9626-9630.

Fujiwara K, Adachi H, Nishio T, Unno M, Tokui T, Okabe M, Onogawa T, Suzuki T, Asano N, Tanemoto M, Seki M, Shiiba K, Suzuki M, Kondo Y, Nunoki K, Shimosegawa T, Iinuma K, Ito S, Matsuno S and Abe T (2001) Identification of thyroid hormone transporters in humans: different molecules are involved in a tissue-specific manner. *Endocrinology* **142**:2005-2012

Hagenbuch B and Meier PJ (2003) The superfamily of organic anion transporting polypeptides. *Biochim Biophys Acta* **1609**:1-18.

Honjo H (1979) Estrogen metabolism and enterohepatic circulation. *Nippon Rinsho* **37**:46-52.

Hsiang B, Zhu Y, Wang Z, Wu Y, Sasseville V, Yang WP and Kirchgessner TG (1999) A novel human hepatic organic anion transporting polypeptide (OATP-2). *J Biol Chem* **274**:37161-37168.

Ishikawa T, Tsuji A, Inui K, Sai Y, Anzai N, Wada M, Endou H, Sumino Y (2004) The genetic polymorphism of drug transporters: Functional analysis approaches. *Pharmacogenomics* **5**:67-99.

Janecki AJ, Montrose MH, Zimnial P, Zweibaum A, Tse CM, Lhurana S and Donowitz M (1998) Subcellular redistribution is involved in acute regulation of the brush border Na^+/H^+ exchanger isoform 3 in human colon adenocarcinoma cell line Caco-2. *J Biol Chem* **273**:8790-8798.

Kobayashi D, Nozawa T, Imai K, Nezu J, Tsuji A and Tamai I (2003) Involvement of human organic anion transporting polypeptide OATP-B (SLC21A9) in pH-dependent transport across intestinal apical membrane. *J Pharmacol Exp Ther* **306**:703-708.

König J, Cui Y, Nies AT and Keppler D (2000) Localization and genomic organization of a new hepatocellular organic anion transporting polypeptide. *J Biol Chem* **275**:23161-23168.

Kullak-Ublick GA, Ismair MG, Stieger B, Landmann L, Huber R, Pizzagalli F, Fattinger K and Meier PJ (2001) Organic anion-transporting polypeptide B (OATP-B) and its functional comparison with three other OATPs of human liver. *Gastroenterology* **120**:525-533.

Lu R, Kanai N, Bao Y and Schuster VL (1996) Cloning, in vitro expression, and tissue distribution of a human prostaglandin transporter cDNA(hPGT). *J Clin Invest* 98:1142-1149.

Mikkaichi T, Suzuki T, Onogawa T, Tanemoto M, Mizutamari H, Okada M, Chaki T, Masuda S, Tokui T, Eto N, Abe M, Satoh F, Unno M, Hishinuma T, Inui K, Ito S, Goto J, Abe T. (2004) Isolation and characterization of a digoxin transporter and its rat homologue expressed in the kidney. *Proc Natl Acad Sci USA* **101**: 3569-3574.

Naruhashi K, Sai Y, Tamai I, Suzuki N and Tsuji A (2002) PepT1 mRNA expression is induced by starvation and its level correlates with absorptive

transport of cefadroxil longitudinally in the rat intestine. *Pharm Res* **19**:1417-1423.

Nozawa T, Nakajima M, Tamai I, Noda K, Nezu J, Sai Y, Tsuji A and Yokoi T (2002) Genetic polymorphisms of human organic anion transporters OATP-C (SLC21A6) and OATP-B (SLC21A9): allele frequencies in the Japanese population and functional analysis. *J Pharmacol Exp Ther* **302**:804-813.

Nozawa T, Imai K, Nezu J, Tsuji A and Tamai I (2004) Functional characterization of pH-sensitive organic anion transporting polypeptide OATP-B in human. *J Pharmacol Exp Ther* **308**: 438-445.

Pizzagalli F, Hagenbuch B, Stieger B, Klenk U, Folkers G and Meier PJ (2002) Identification of a novel human organic anion transporting polypeptide as a high affinity thyroxine transporter. *Mol Endocrinol* **16**:2283-2296.

Pizzagalli F, Varga Z, Huber RD, Folkers G, Meier PJ and St-Pierre MV (2003) Identification of steroid sulfate transport processes in the human mammary gland. *J Clin Endocrinol Metab* **88**:3902-3912.

Saeki T, Matoba K, Furukawa H, Kirifuji K, Kanamoto R, Iwami K (1999) Characterization, cDNA cloning, and functional expression of mouse ileal sodium-dependent bile acid transporter. *J Biochem (Tokyo)* **125**:846-851.

Shiau YF, Fernandez P, Jackson MJ and McMonagle S (1985) Mechanisms maintaining a low-pH microclimate in the intestine. *Am J Physiol*

248:G608-G617.

Stelzner M, Hoagland V, Somasundaram S (2000) Distribution of bile acid absorption and bile acid transporter gene message in the hamster ileum. *Pflugers Arch* **440**:157-162.

St-Pierre MV, Hagenbuch B, Ugele B, Meier PJ and Stallmach T (2002) Characterization of an organic anion-transporting polypeptide (OATP-B) in human placenta. *J Clin Endocrinol Meatb* **87**:1856-1863

Sun D, Lennernas H, Welage LS, Barnett JL, Landowski CP, Foster D, Fleisher D, Lee KD and Amidon GL (2002) Comparison of human duodenum and Caco-2 gene expression profiles for 12,000 gene sequences tags and correlation with permeability of 26 drugs. *Pharm Res* **19**:1400-1416.

Taipalensuu J, Tornblom H, Lindberg G, Einarsson C, Sjoqvist F, Melhus H, Garberg P, Sjostrom B, Lundgren B and Artursson P (2001) Correlation of gene expression of ten drug efflux proteins of the ATP-binding cassette transporter family in normal human jejunum and in human intestinal epithelial Caco-2 cell monolayers. *J Pharmacol Exp Ther* **299**:164-170.

Tamai I, Takanaga H, Maeda H, Ogihara T, Yoneda M and Tsuji A (1995) Proton-cotransport of pravastatin across intestinal brush-border membrane. *Pharm Res* **12**:1727-1732.

Tamai I, Takanaga H, Maeda H, Yabuuchi H, Sai Y, Suzuki Y and Tsuji A (1996) Intestinal brush-border membrane transport of monocarboxylic acids

mediated by proton-coupled transport and anion antiport mechanism. *J Pharm Pharmacol* **49**:108-112.

Tamai I, Sai Y, Ono A, Kido Y, Yabuuchi H, Takanaga H, Satoh E, Ogihara T, Amano O, Iseki S and Tsuji A (1999) Immunohistochemical and functional characterization of pH-dependent intestinal absorption of weak organic acids by the monocarboxylic acid transporter MCT1. *J Pharm Pharmacol* **51**:1113-1121.

Tamai I, Nezu J, Uchino H, Sai Y, Oku A, Shimane M and Tsuji A (2000a) Molecular identification and characterization of novel members of the human organic anion transporter (OATP) family. *Biochem Biophys Res Commun* **273**:251-260.

Tamai I, Ogihara T, Takanaga H, Maeda H and Tsuji A (2000b) Anion antiport mechanism is involved in transport of lactic acid across intestinal epithelial brush-border membrane. *Biochem Biophys Acta* **1468**:285-292.

Tamai I, Nozawa T, Koshida M, Nezu J, Sai Y and Tsuji A (2001a) Functional characterization of human organic anion transporting polypeptide B (OATP-B) in comparison with liver-specific OATP-C. *Pharm Res* **18**:1262-1269.

Tamai I, China K, Sai Y, Kobayashi D, Nezu J, Kawahara E. and Tsuji A. (2001b) Na^+-coupled transport of L-carnitine via high-affinity carnitine transporter OCTN2 and its subcellular localization in kidney. *Biochim Biophys Acta*

1512:273-284.

Tavelin S, Grasjo J, Taipalensuu J, Ocklind G and Artursson P (2002) Applications of epithelial cell culture in studies of drug transport. *Methods Mol Biol* **188**:233-272.

Thwaites DT, Kennedy DJ, Raldua D, Anderson CM, Mendoza ME, Bladen CL and Simmons NL (2002) H^+/dipeptide absorption across the human intestinal epithelium is controlled indirectly via a functional Na^+/H^+ exchanger. *Gastroenterology* **122**:1322-1333.

Ugele B, St-Pierre MV, Pihusch M, Bahn A and Hantschmann P (2003) Characterization and identification of steroid sulfate transporters of human placenta. *Am J Physiol* **284**:E390-398.

Walker D, Thwaites DT, Simmons NL, Gilbert HJ and Hirst BH (1998) Substrate upregulation of the human small intestinal peptide transporter, hPepT1. *J Physiol* **507**:697-706.

Watanabe C, Kato Y, Ito S, Kubo Y, Sai Y and Tsuji A (2005) Na^+/H^+ exchanger 3 affects transport property of H^+/oligopeptide transporter 1. *Drug Metab Pharmacokinet* **20**:443-451.

Yamaoka K, Tanigawara Y, Nakagawa T and Uno T (1981) A pharmacokinetic analysis program (MULTI) for microcomputer. *J Pharmacobiodyn* **4**:879-885.

Footnotes

a)

***** This work was supported in part by a grant-in-aid for scientific research from the Ministry of Education, Science, Sports, and Culture of Japan.

b)

Akira Tsuji, Ph.D., Professor

Division of Pharmaceutical Sciences, Graduate School of Natural Science and Technology, Kanazawa University

Kakuma-machi, Kanazawa, Ishikawa 920-1192, Japan

tsuji@kenroku.kanazawa-u.ac.jp

DMD Fast Forward. Published on May 19, 2006 as DOI: 10.1124/dmd.106.009530
This article has not been copyedited and formatted. The final version may differ from this version.

Legends for Figures

Figure 1

Confocal Laser Scaning Microscopic Analysis of Immunocytochemical Localization of OATP-B Protein in Caco-2 Cells

(A) Immunocytochemical detection of OATP-B (red) and Na^+/K^+-ATPase (green) in Caco-2 cell monolayers was performed using anti-OATP-B antibody (a-c) or rabbit normal IgG (d-f) and anti-Na^+/K^+-ATPase antibody (a-f) as a basolateral marker. Images (x-y sections) were taken through Caco-2 cell monolayers from the apical to basal surfaces: at the apical surface (a, d), 5.1 μm below the apical surface (b, e) and 11 μm below the apical surface (c, f) of the monolayers. The scale bar represents 10 μm. (B) Side view (X-Z reconstruction) showing localization of OATP-B and Na^+/K^+-ATPase in each monolayer. The upper and lower sides of the images represent the apical and basal cell membranes, respectively. a, Double staining with anti-OATP-B and anti-Na^+/K^+-ATPase antibodies; b, Double staining with rabbit normal IgG and anti-Na^+/K^+-ATPase antibody. The secondary antibodies used were Alexa 488-labeled goat anti-mouse IgG and Alexa 594-labeled goat anti-rabbit IgG.

Figure 2

RT-PCR and Western Blot Analysis of OATP-B in HEK293/OATP-B,

HEK293/Mock and Caco-2 Cells

(A) RT-PCR using specific primers for OATP-B was performed with total RNA prepared from HEK293/OATP-B (lane 1, 2), HEK293/Mock (lane 3, 4) and Caco-2 cells (lane 5, 6). Reverse transcription was performed in the presence (lane 1, 3, 5) or absence (lane 2, 4, 6) of reverse transcriptase. PCR products were separated by 2% agarose gel electrophoresis, followed by staining with ethidium bromide. (B) Crude membrane fraction was prepared from HEK293/OATP-B (lane 1) and Caco-2 (lane 2, 3) cells followed by treatment with peptide *N*-glycosidase F to remove sugar modification (lane 1, 3). Each of the protein samples was subjected to SDS-PAGE and immunoblotting using anti-OATP-B antibody. M, molecular weight marker.

Figure 3

Time Course of Uptake of [^{3}H]Estrone-3-sulfate by HEK293/OATP-B, HEK293/Mock and Caco-2 Cells

Uptake of [^{3}H]estrone-3-sulfate (4.7 nM) by HEK293/OATP-B or HEK293/Mock cells over 10 min was measured at 37 °C in the uptake medium at pH 6.0 (A) or pH 7.4 (B) after preincubation for 20 min at 37 °C in the incubation medium (pH 7.4). Uptake of [^{3}H]estrone-3-sulfate (4.7 nM) by Caco-2 cells over 30 min was measured at 37 °C in the uptake medium at pH 6.0 (C) or pH 7.4 (D) after preincubation for 10 min at 37 °C in the incubation medium (pH 7.4). Closed

and open circles represent the uptake in the absence or presence of unlabeled (100 μM for HEK293 and 4 mM for Caco-2 cells) estrone-3-sulfate, respectively. Closed and open triangles represent the corresponding values for HEK293/Mock cells (A, B). Each result represents the mean ± S.E.M. (n = 4). * Significantly different from the value measured in the presence of unlabeled estrone-3-sulfate ($p < 0.05$).

Figure 4

Effects of Extracellular Cations on Uptake of [^{3}H]Estrone-3-sulfate by HEK293/OATP-B (A) and Caco-2 (B) Cells

(A) HEK293/OATP-B cells were preincubated for 20 min at 37 °C in the incubation medium (pH 7.4). Uptake of [^{3}H]estrone-3-sulfate (4.7 nM) over 2 min was then measured at 37 °C by incubating cells in the uptake medium at pH 6.0. The results were normalized by the uptake in the presence of Na^+ after correcting for the uptake by HEK293/Mock cells. Each result represents the mean ± S.E.M. (n = 4). (B) Caco-2 cells were preincubated for 10 min at 37 °C in the incubation medium (pH 7.4). Uptake of [^{3}H]estrone-3-sulfate (4.7 nM) over 2 min was then measured at 37 °C by incubating cells in the uptake medium at pH 6.0. The results were normalized by the uptake in the presence of Na^+. Each result represents the mean ± S.E.M. (n = 3). * Significantly different from the control ($p < 0.05$).

DMD Fast Forward. Published on May 19, 2006 as DOI: 10.1124/dmd.106.009530
This article has not been copyedited and formatted. The final version may differ from this version.

Figure 5

Concentration Dependence of Uptake of [^{3}H]Estrone-3-sulfate by HEK293/OATP-B, HEK293/Mock and Caco-2 Cells

(A) Uptake of estrone-3-sulfate at various concentrations for 2 min was measured at pH 6.0 and 37 °C in HEK293/OATP-B (closed circles) and HEK293/Mock (open circles) cells. Dotted and solid lines represent nonsaturable uptake observed in HEK293/Mock cells and saturable uptake mediated by OATP-B, respectively, both of which were obtained from nonlinear least-squares regression analysis as described in Materials and Methods. Each result represents the mean ± S.E.M. (n = 4). (B) OATP-B-mediated uptake of estrone-3-sulfate at various concentrations at pH 6.0 is shown as an Eadie-Hofstee plot. The straight line was obtained by fitting based on nonlinear least-squares regression analysis.

(C) Uptake of estrone-3-sulfate at various concentrations for 2 min was measured at pH 6.0 and 37 °C. Dotted and solid lines represent the nonsaturable and saturable uptake, respectively, obtained from nonlinear least-squares regression analysis of the total uptake (closed circles). Each result represents the mean ± S.E.M. (n = 3). (D) Saturable uptake of estrone-3-sulfate is shown as an Eadie-Hofstee plot. The straight line was obtained by fitting based on nonlinear least-squares regression analysis.

Figure 6

Inhibitory Effect of BSP (Open Circles), DHEAS (Closed Circles), Pravastatin (Open Squares) and Benzylpenicillin (Closed Squares) on Uptake of [^{3}H]Estrone-3-sulfate by HEK293/OATP-B and Caco-2 Cells

(A) HEK293/OATP-B cells were preincubated for 20 min at 37 °C in the incubation medium (pH 7.4). Uptake of [^{3}H]estrone-3-sulfate (4.7 nM) was then measured for 2 min at 37 °C by incubating cells in the uptake medium at pH 6.0. The results are shown as a percentage of control uptake after correcting for the uptake by HEK293/Mock cells. Each result represents the mean ± S.E.M. (n = 4). (B) Caco-2 cells were preincubated for 10 min at 37 °C in the incubation medium (pH 7.4). Uptake of [^{3}H]estrone-3-sulfate (4.7 nM) over 2 min was then measured at 37 °C by incubating cells in the uptake medium at pH 6.0. The results are shown as percentage of control uptake. Each result represents the mean ± S.E.M. (n = 3).

Figure 7

Inhibitory Effect of Various Compounds on Uptake of [^{3}H]Estrone-3-sulfate by HEK293/OATP-B and Caco-2 Cells

(A) HEK293/OATP-B cells were preincubated for 20 min at 37 °C in the incubation medium (pH 7.4). Uptake of [^{3}H]estrone-3-sulfate (4.7 nM) was then

measured for 2 min at 37 °C or 4 °C by incubating cells in the uptake medium at pH 6.0. The results are shown as a percentage of control uptake after correcting for the uptake by HEK293/Mock cells. Each result represents the mean ± S.E.M. (n = 4). (B) Caco-2 cells were preincubated for 10 min at 37 °C in the incubation medium (pH 7.4). Uptake of [^{3}H]estrone-3-sulfate (4.7 nM) over 2 min was then measured at 37 °C or 4 °C by incubating cells in the uptake medium at pH 6.0. The results are shown as a percentage of control uptake. Each result represents the mean ± S.E.M. (n = 3). * Significantly different from the control ($p < 0.05$).

Figure 8

Initial Uptake Clearance of [^{3}H]Estrone-3-sulfate and mRNA Expression of OATP-B, OATP-D and OATP-E in Caco-2 Cells and HEK293 Cells Expressing OATP-B, OATP-D and OATP-E

Initial uptake clearance of [^{3}H]estrone-3-sulfate (4.7 nM) and mRNA expression level of OATP-B (circles), OATP-D (triangle) or OATP-E (square) were measured in HEK293 cells transiently transfected with OATP-B, OATP-D or OATP-E cDNA in various amounts of plasmid. For comparison, uptake clearance of [^{3}H]estrone-3-sulfate in Caco-2 cells is shown as a broken line. mRNA expression levels of OATP-B, OATP-D or OATP-E in Caco-2 cells are shown with arrows: (B), (D) or (E), respectively. The gray bar represents

DMD Fast Forward. Published on May 19, 2006 as DOI: 10.1124/dmd.106.009530
This article has not been copyedited and formatted. The final version may differ from this version.

non-saturable transport of [^{3}H]estrone-3-sulfate in Caco-2 and HEK293 cells.

Figure 9

Effect of an H^+-gradient on Uptake of [^{3}H]Estrone-3-sulfate by Membrane Vesicles Obtained from HEK293/OATP-B and HEK293/Mock

Membrane vesicles obtained from HEK293/OATP-B (circles) or HEK293/Mock cells (triangles) were preincubated for 10 min at 37 °C in the transport buffer (pH 7.4). Uptake of [^{3}H]estrone-3-sulfate (47 nM) was then measured over 120 min at pH 6.0 (A) or pH 7.4 (B) in the absence (closed symbols) or presence (open symbols) of 50 µM FCCP. Each point represents the mean and S.E.M. (n = 3). * Significantly different from mock-vesicles ($p < 0.05$).

DMD Fast Forward. Published on May 19, 2006 as DOI: 10.1124/dmd.106.009530
This article has not been copyedited and formatted. The final version may differ from this version.

Table 1

mRNA Expression Level of OATP-B, OATP-D, OATP-E and Villin in Human Jejunal Biopsy Sample and Caco-2 Cells Examined by Quantitative Real-Time PCR Analysis

Subject No	mRNA Expression Level (copy/ng total RNA)				Ratio
	OATP-B	OATP-D	OATP-E	Villin	OATP-B/Villin
1	120	29	3.5	500	0.24
2	327	100	14.6	942	0.35
3	317	112	10.0	544	0.58
4	254	83	5.9	746	0.34
5	406	73	6.8	795	0.51
6	207	46	3.2	462	0.45
7	414	74	6.4	545	0.76
9	469	73	9.5	838	0.56
10	164	41	8.1	564	0.29
11	239	112	9.7	751	0.32
12	183	62	9.5	563	0.33
13	102	77	9.0	750	0.14
14	751	74	12.0	597	1.26
Mean	304	74*	8.3*	661	0.47
S.D. (n = 13)	177	25	3.2	149	0.29
Caco-2 cells (Mean, n = 2)	9,030	34.9	154	925	9.76

* Significantly different from OATP-B ($p < 0.05$).

DMD Fast Forward. Published on May 19, 2006 as DOI: 10.1124/dmd.106.009530
This article has not been copyedited and formatted. The final version may differ from this version.

Table 2

IC_{50} Values for the Inhibitory Effects of Typical Substrates of OATP-B on Uptake of [^{3}H]Estrone-3-sulfate by HEK293/OATP-B and Caco-2 cells

	IC_{50}*		
Compounds	HEK293/OATP-B	Caco-2	
BSP	0.282 ± 0.062	2.89 ± 0.74	(μM)
DHEAS	8.60 ± 0.37	12.0 ± 3.4	(μM)
Pravastatin	1.02 ± 0.10	1.06 ± 0.11	(mM)
Benzylpenicillin	16.0 ± 3.4	10.2 ± 1.6	(mM)

* Each data represents the mean ± S.E.M. (n = 3).

Figure 1

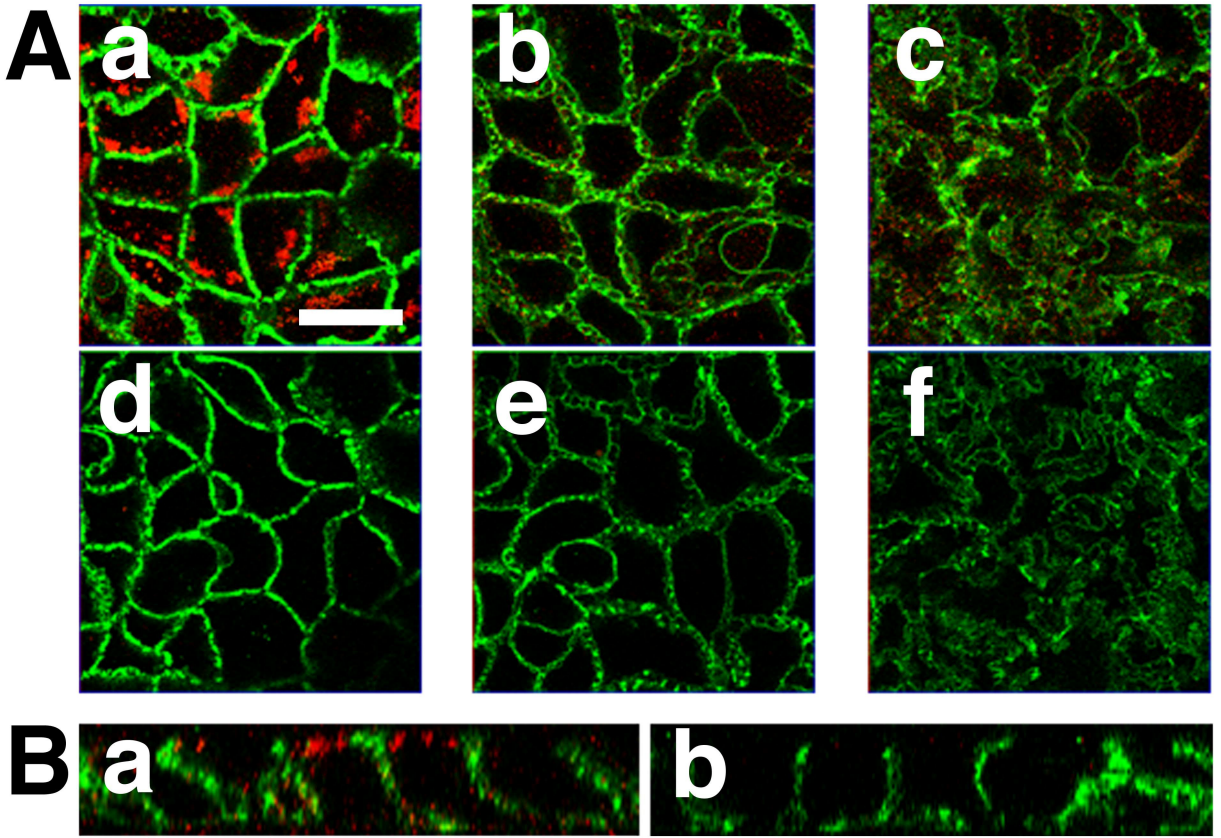

Figure 2

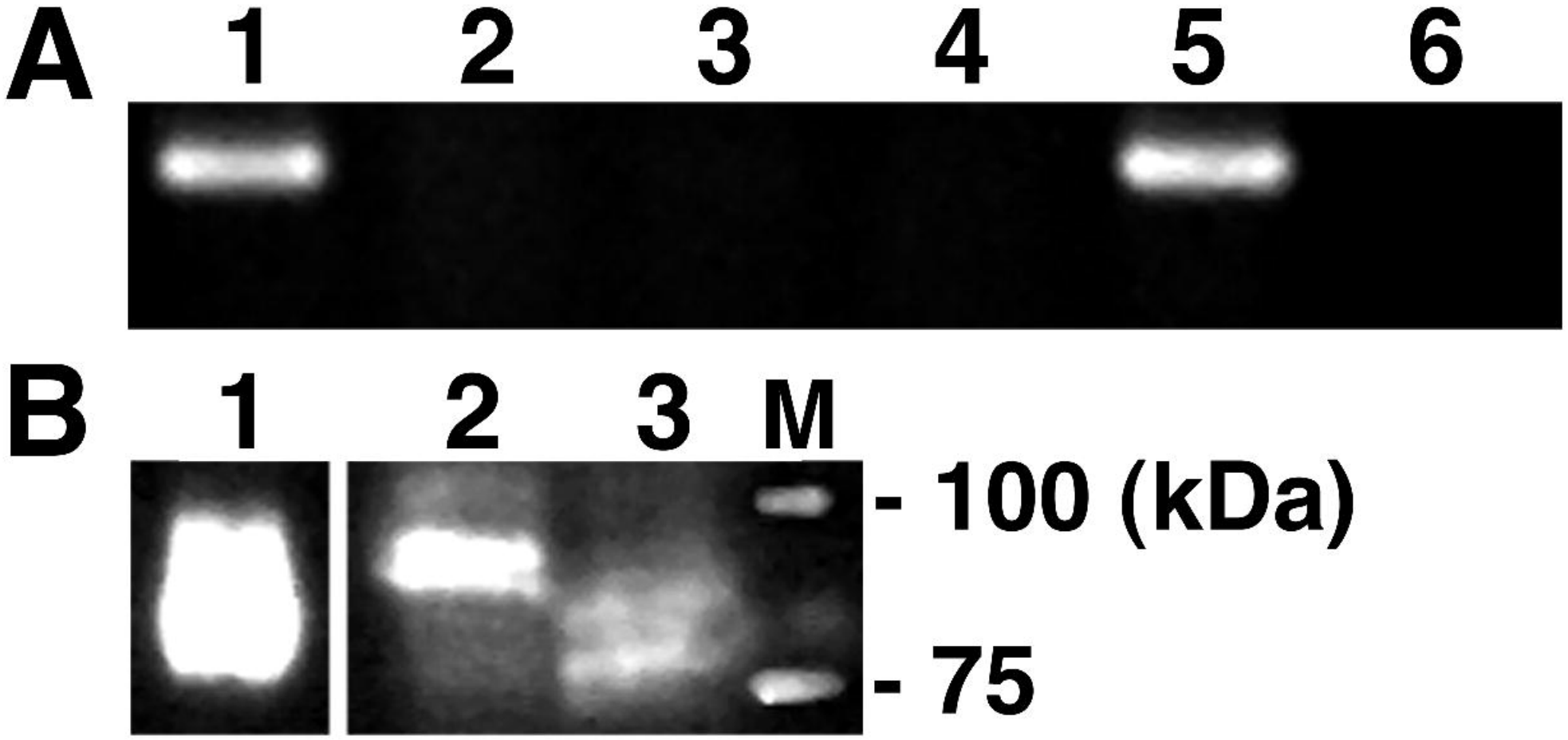

Figure 3

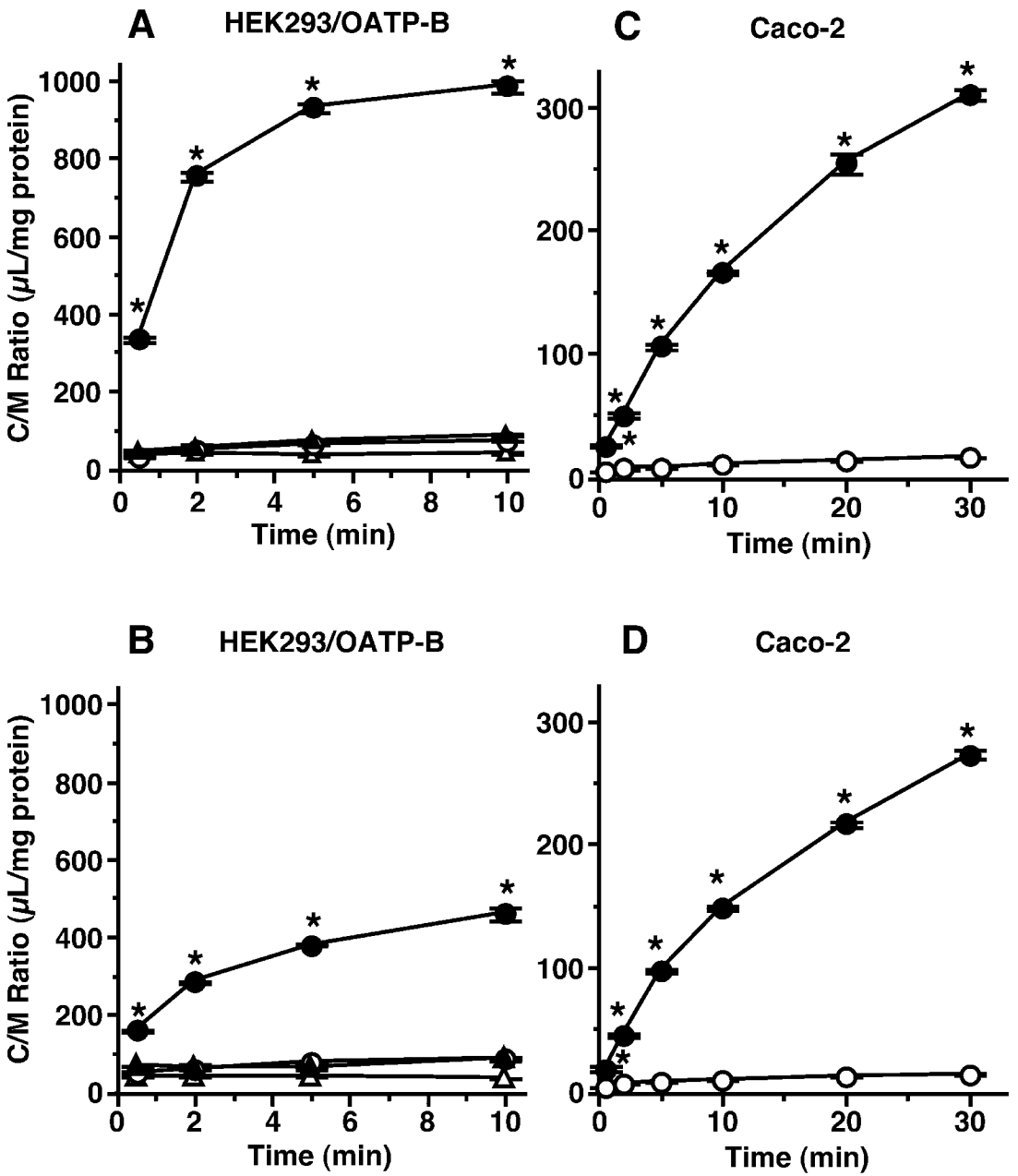
A
HEK293/OATP-B
C
Caco-2
B
HEK293/OATP-B
D
Caco-2
C/M Ratio (μL/mg protein)
Time (min)
0
200
400
600
800
1000
100
300
2
4
6
8
10
20
30
*

Figure 4

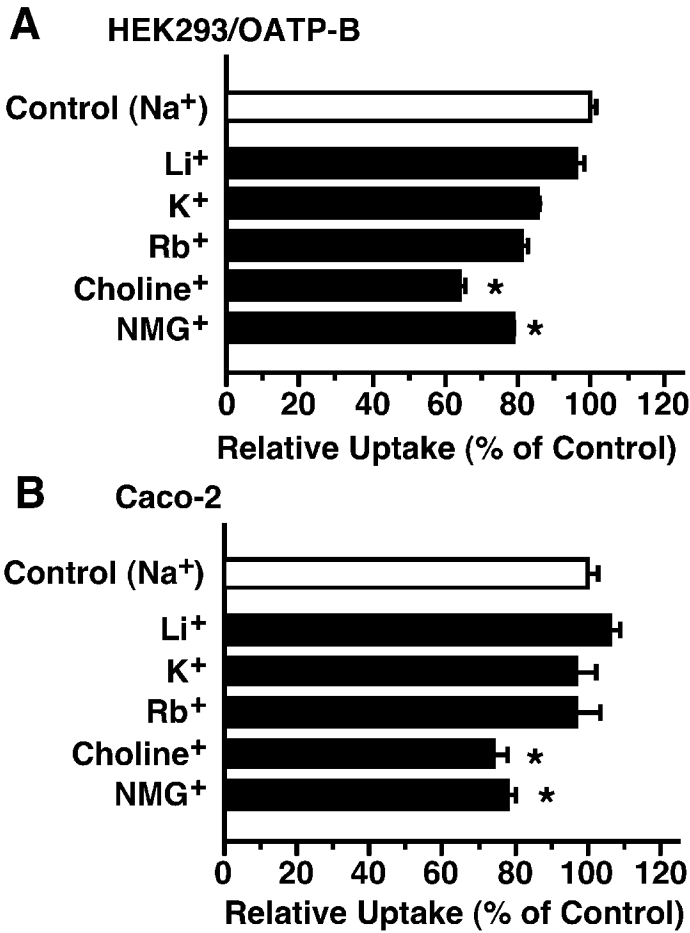
A
HEK293/OATP-B
Control (Na+)
Li+
K+
Rb+
Choline+
NMG+
*
*
0
20
40
60
80
100
120
Relative Uptake (% of Control)
B
Caco-2
Control (Na+)
Li+
K+
Rb+
Choline+
NMG+
*
*
0
20
40
60
80
100
120
Relative Uptake (% of Control)

Figure 5

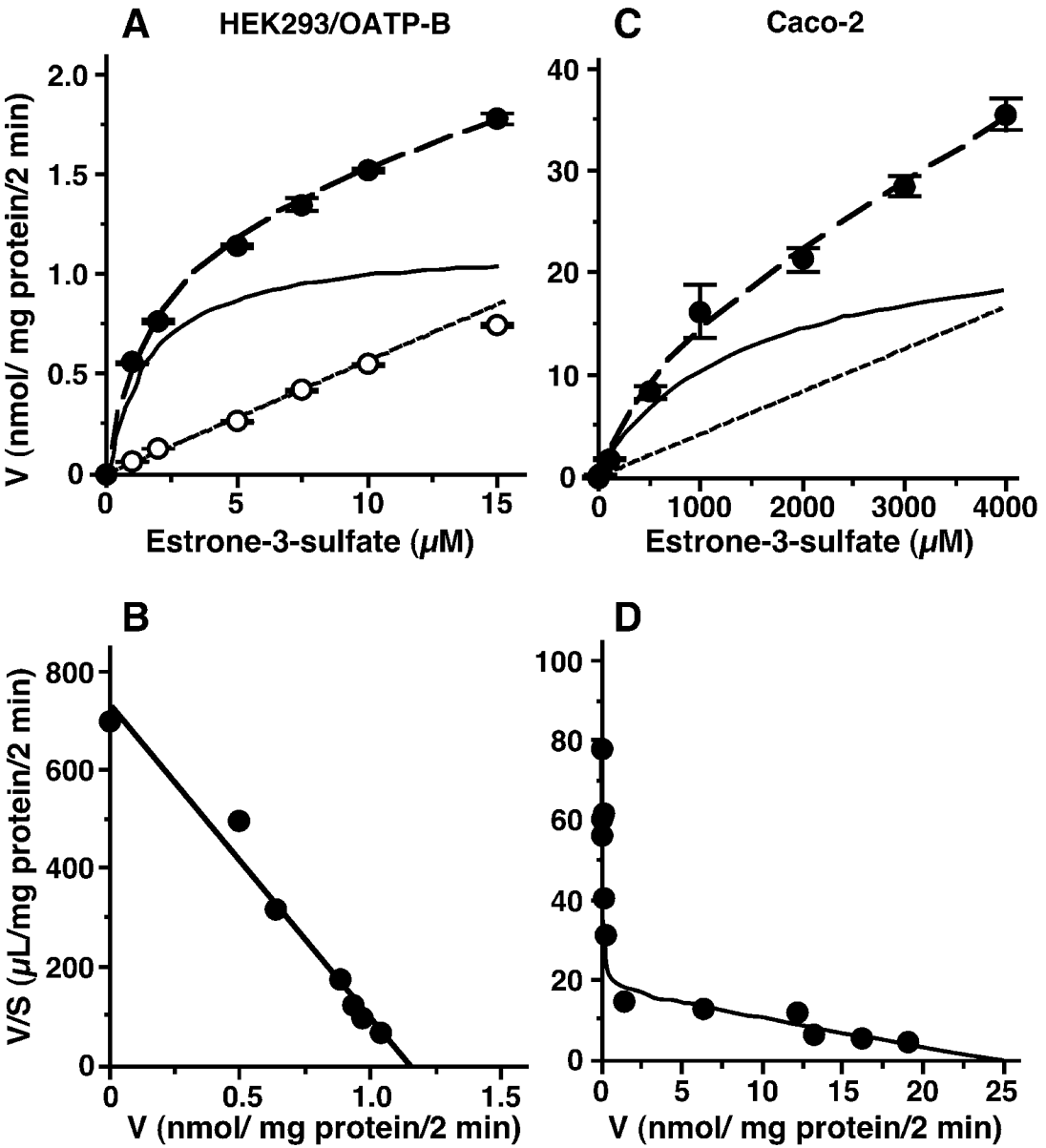
A
HEK293/OATP-B
V (nmol/ mg protein/2 min)
Estrone-3-sulfate (μM)
C
Caco-2
Estrone-3-sulfate (μM)
B
V/S (μL/mg protein/2 min)
V (nmol/ mg protein/2 min)
D
V (nmol/ mg protein/2 min)

Figure 6

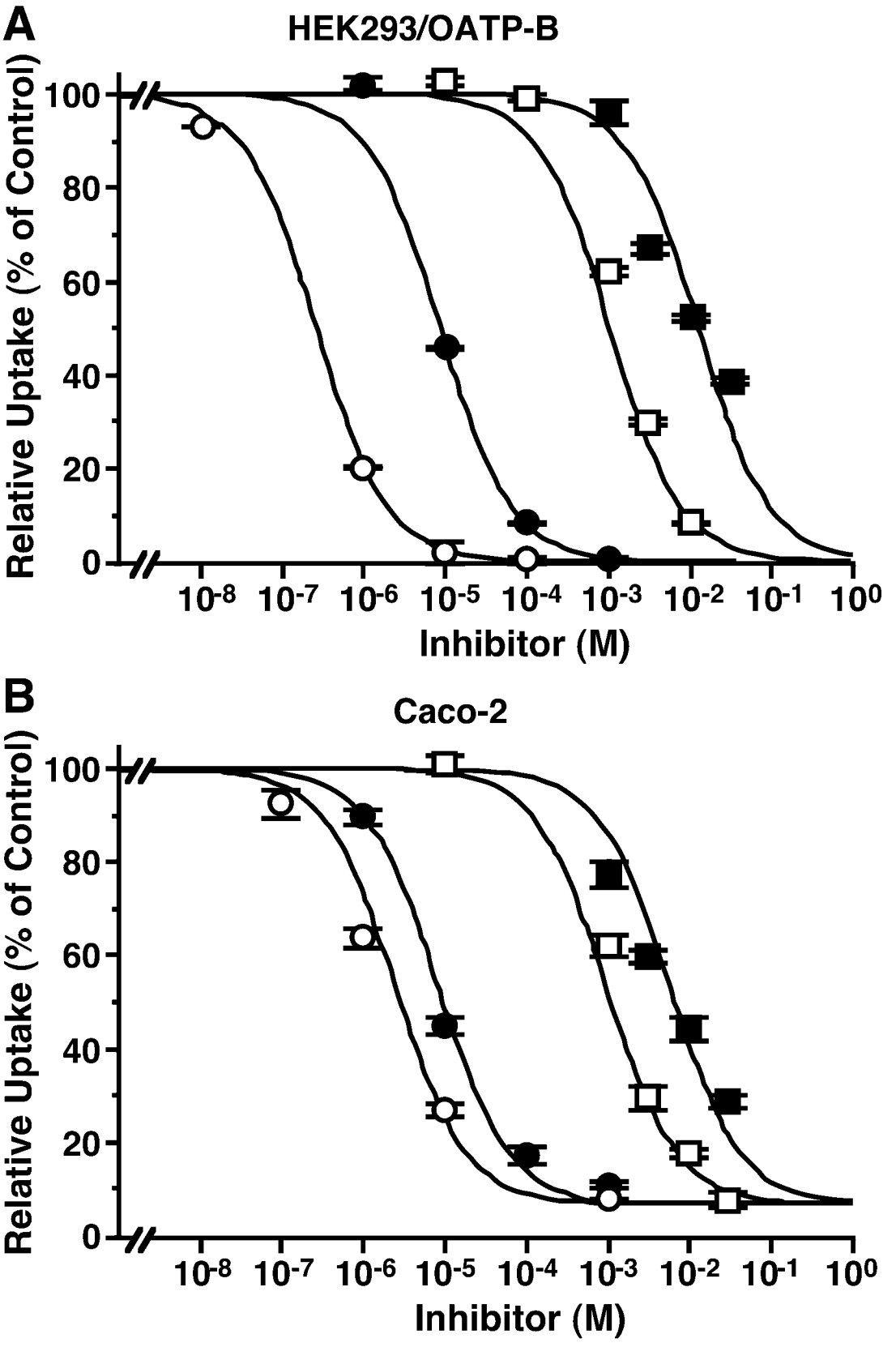
A
HEK293/OATP-B
Relative Uptake (% of Control)
100
80
60
40
20
0
10-8 10-7 10-6 10-5 10-4 10-3 10-2 10-1 100
Inhibitor (M)
B
Caco-2
Relative Uptake (% of Control)
100
80
60
40
20
0
10-8 10-7 10-6 10-5 10-4 10-3 10-2 10-1 100
Inhibitor (M)

Figure 7

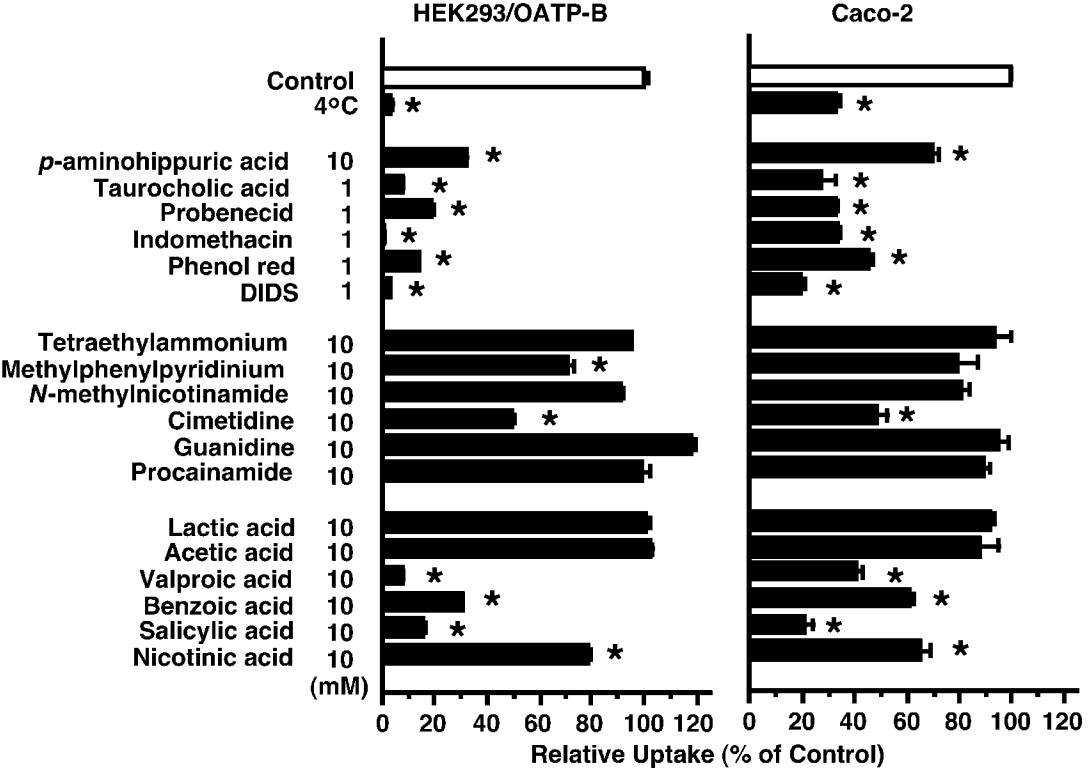
HEK293/OATP-B
Caco-2
Control
4°C
p-aminohippuric acid 10
Taurocholic acid 1
Probenecid 1
Indomethacin 1
Phenol red 1
DIDS 1
Tetraethylammonium 10
Methylphenylpyridinium 10
N-methylnicotinamide 10
Cimetidine 10
Guanidine 10
Procainamide 10
Lactic acid 10
Acetic acid 10
Valproic acid 10
Benzoic acid 10
Salicylic acid 10
Nicotinic acid 10
(mM)
0 20 40 60 80 100 120
0 20 40 60 80 100 120
Relative Uptake (% of Control)

Figure 8

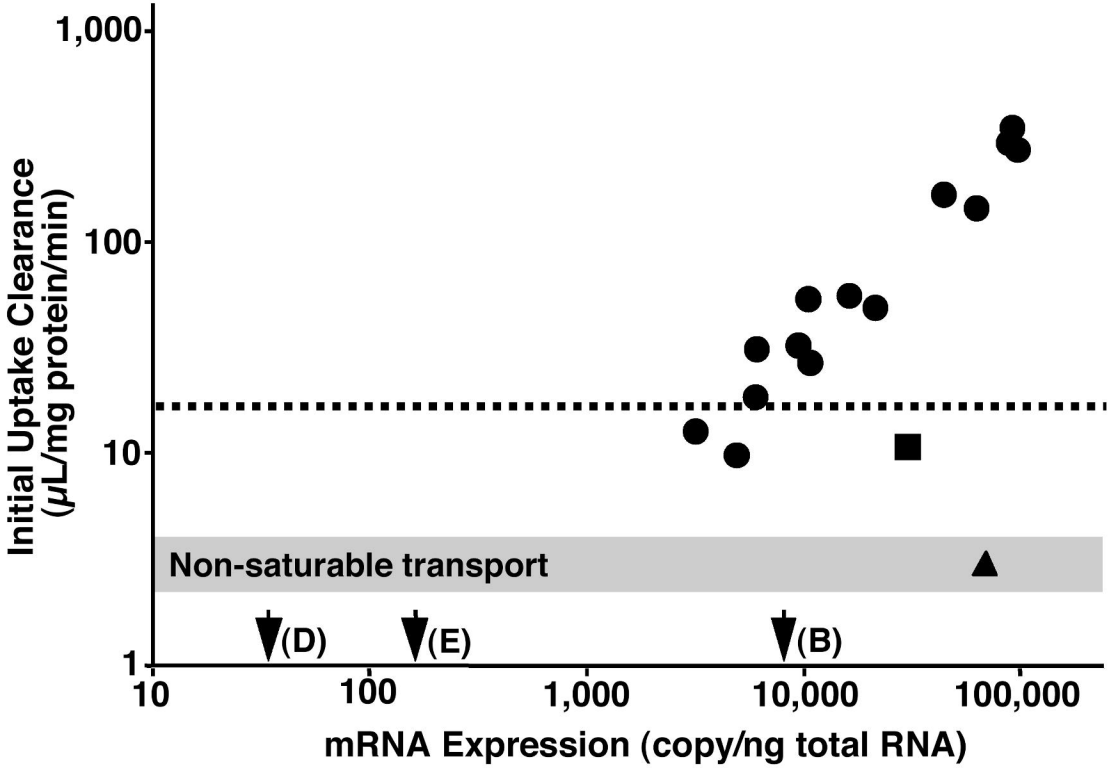
1,000
100
10
1
Initial Uptake Clearance
(μL/mg protein/min)
Non-saturable transport
(D)
(E)
(B)
10
100
1,000
10,000
100,000
mRNA Expression (copy/ng total RNA)

Figure 9